Carbohydrate Polymers 272 (2021) 118455

Contents lists available at ScienceDirect

Carbohydrate Polymers

journal homepage: www.elsevier.com/locate/carbpol

Impact of drying on the sodium alginate obtained after polyphenols ultrasound-assisted extraction from *Ascophyllum nodosum* seaweeds

Leticia Montes, Mauro Gisbert, Ignacio Hinojosa, Jorge Sineiro, Ramón Moreira *

Department of Chemical Engineering, Universidade de Santiago de Compostela, rúa Lope Gómez de Marzoa, Santiago de Compostela E-15782, Spain

ARTICLE INFO

Keywords:
FT-IR
NMR
Rheology
UAE
Viscosity average molecular weight

ABSTRACT

Ultrasound-assisted extraction (UAE) of polyphenols from the brown seaweeds *Ascophyllum nodosum* leaves a solid phase where alginates can be extracted. This study characterizes alginates extracted after the UAE process, with and without an intermediate drying stage at different temperatures (50 and 90 °C) producing sequentially two bioactive compounds from a unique raw material. FT-IR and ^{1}H NMR analyses showed the high purity of alginates with features in the range of commercial alginates. Drying at high temperature decreased average block length and viscosity average molecular weight (M_v) of alginate from 428 to 133 kg/mol. Steady-shear curves (shear-thinning behaviour) and viscoelasticity (liquid like character) features depended clearly on M_v. Solutions of alginates with high M_v were more viscous and the elastic character was more relevant. Cox-Merz rule was only accomplished within the semi-dilute regimes of alginate concentration. Tested process conditions allow the production of alginates with different properties.

1. Introduction

Alginate is a polyuronan isolated from some seaweeds or produced by some bacterial species. Alginate is mainly present in brown algae species (*Phaeophyceae*) being a structural component of the matrix cell wall and responsible of seaweed flexibility and mechanical resistance (Donati & Paoletti, 2009). Its industrial exploitation is mainly focused on 38 seaweeds species (Peteiro, 2018), among which stands out *Ascophyllum nodosum* (AN).

Alginates are linear binary copolymers of linked by 1–4-glycosidic bonds. Alginate monomers are α-L-guluronate (G), and β-D-mannuronate (M), Fig. 1. M/G ratio value measures M and G-blocks distribution along alginate molecules (Gómez-Ordóñez & Rupérez, 2011), and $N_{G>1}$ values measure the average block length (ASTM, 2012). M/G and $N_{G>1}$ values vary among species, within the different parts of an organism, life stages of seaweeds, and extraction and isolation procedures. M/G ratio, among other properties, can be used as an index for the alginate gels physical properties, for example, lower values (<1) produce strong gels. These versatile properties make that alginates can cover a wide spectrum of industrial applications (Gómez-Ordóñez & Rupérez, 2011).

Alginates have many industrial applications by their thickening, emulsifying, and stabilizing properties mainly in food industry, but non-food uses are also important like dye, biomaterials, medical and pharmaceutical industries (Donati & Paoletti, 2009). The selection of the optimal alginates according to the uses that it will be given is closely conditioned by their features such as chemical structure, molecular size, or chemical composition, making that alginates characterization a mandatory task. Alginates are highly sensitive to temperature, pH and contaminants presence as the presence of free radicals, promoted by some polyphenols, co-extracted during alginate isolation. Particularly, free radicals could reduce alginate molecular weight since enhance depolymerization and oxidation-reduction reactions. These reactions are promoted by low pH values and high temperature (Donati & Paoletti, 2009).

Alginates extraction process from marine algae is based on the conversion of the alginic acid from the cell wall into alginate salt forms, followed by precipitation and purification steps. Firstly, seaweeds are washed, dried and grounded. Formaldehyde can be added to remove coloured matter. Milled seaweeds are soaked in dilute acidic solutions to remove fucoidans, laminarins, proteins and polyphenols that could modify alginate features. Then, alginic acid is transformed into sodium alginate employing alkaline solutions. Solid residues are removed by

* Corresponding author at: Department of Chemical Engineering, Universidade de Santiago de Compostela, rúa Lope Gómez de Marzoa, Santiago de Compostela E-15782, Spain.
E-mail addresses: leticia.montes.martinez@usc.es (L. Montes), mauro.gisbert.verdu@usc.es (M. Gisbert), ignacio.hinojosa@rai.usc.es (I. Hinojosa), jorge.sineiro@usc.es (J. Sineiro), ramon.moreira@usc.es (R. Moreira).

https://doi.org/10.1016/j.carbpol.2021.118455
Received 26 April 2021; Received in revised form 9 July 2021; Accepted 15 July 2021
Available online 20 July 2021

centrifugation and filtration. Then, alginate is precipitated with ethanol to obtain sodium alginate (Chee et al., 2011; Donati & Paoletti, 2009). Other alginates can be also produced such as calcium alginate, alginic acid, potassium alginate or ammonium alginate using alternatives to alkaline solution (Peteiro, 2018).

Polyphenols and other algae coloured compounds (chlorophyl, carotenoids) produce a brown discoloration, during alkaline treatment, resulting in an unpleasing dark sodium alginate powder. Bleaching pretreatments fix these coloured compounds to algae tissues reducing brown discoloration, but critically affect the rheological, chemical, and structural features of alginates by modification of molecular weight and M/G ratio (Mohammed et al., 2020). Nowadays, there is a growing interest in isolating polyphenols for their own unique bioactivity characteristics from algae for various uses (Cotas et al., 2020). A suitable strategy for the transformation of current single-product manufacturing process into biorefineries would be the sequential extraction. Firstly, polyphenols, promising bioactive molecules by their antioxidant properties and potential applications as enzymatic inhibitors, anti-inflammatory, and anti-viral properties, among others (Koivikko et al., 2005), and, secondly, alginates that employs more severe conditions. To preserve the polyphenols features and to enhance extraction yields, the use of ultrasound-assisted extraction is a promising, efficient, low-cost, and eco-friendly technology (Kadam et al., 2015).

The novelty of this study is to contribute to the integral valorisation of brown seaweeds, by means of the use the solid residue, after the ultrasound-assisted extraction (UAE) of polyphenols from AN seaweed, that still contains other active components, such as alginate. Sodium alginates thus obtained have not been characterized (to our best knowledge). Consequently, the aim is to determine the effect of the process (existence of a drying stage) and operational conditions (drying temperature) on physicochemical properties of alginates. Alginates are characterized by FT-IR, ^{1}H NMR and viscometric capillary techniques. Rheological studies are carried out to study by rotational and oscillatory tests the viscous character and viscoelastic properties.

2. Materials and methods

2.1. Raw material and reagents

Ascophyllum nodosum (AN) seaweeds harvested from the Galicia's coast (NW of Spain) for autumn season were supplied by Mar de Ardora S.L (Ortigueira, Spain). Samples were washed with running tap water, dried in a hot air convective dryer (Angelantoni, Challenge 250, Italy) at 50 °C, 30% relative humidity and 2 m/s air velocity for 8 h. Dried seaweeds were aerated for 3 days at room temperature (rt, 19 ± 1 °C) to achieve a uniform moisture content (15.5 ± 1.2% dry solid, d.s). Dried seaweeds were milled in an ultra-centrifugal mill (Retsch GmbH, ZM200, Germany) up to achieve flour with a mean particle size of 276 ± 8 μm, determined after vibratory sieving (FTL 0200, Cisa, Spain), using standard meshes from 40 to 500 μm. Seaweed flour was sealed in plastic bags with a vacuum packer and stored at 4 °C until use.

Chemical reagents used in treatments and characterisations were analytical grade. Deuterated water (D_2O), sodium chloride, sodium azide, sodium alginate (CAS no: 9005-38-3, Lot MKCJ1280) from Sigma-Aldrich Inc. (USA). Sodium carbonate, chlorohydric acid, and ethanol from Panreac (Spain).

2.2. Polyphenols ultrasound-assisted extraction (UAE) conditions

Seaweed flour was initially rehydrated with double-distilled water and rested for 15 min before processing. Then, aqueous AN dispersion was sonicated with a nominal 1000 W ultrasound processor (Hielscher, UIP-1000 hdT, Germany) using a 200 mL jacketed chamber. Extraction temperature was controlled with a cold-water bath (Thermo Fisher Scientific, USA) below 30 °C. Continuous UAE operation was performed controlling the liquid flow with a peristaltic pump (Cole Parmer MasterflexTM).

UAE conditions were set to 100% of sonication amplitude ($9{\cdot}10^5$ W/m^2), 120 s of sonication time and 20 kg_W/kg_{DS} of liquid/solid ratio. These operation conditions maximised the polyphenols content (55.6 ± 0.2 g of phloroglucinol equivalents per kg of dried seaweed, g_{PE}/kg_{DS}) of extracts. During UAE, some alginates were also extracted along with polyphenols, 15.2 ± 0.9 g_{GE}/kg_{DS} (g of glucose equivalents per kg of dried seaweed). Polyphenols and alginates content of the extracts were determined following the methods described in Moreira et al. (2016)). The polyphenols-enriched aqueous extract was separated from the solid phase (pellet) by filtration. Pellet was air dried at constant relative humidity (30%), air velocity (2 m/s) at 50 (50D) and 90 °C (90D) for 9.5 h and 3 h, respectively, up to moisture content of 10.8 ± 0.4% (dry basis). Dried pellet was stored at rt. until its use for sodium alginate extraction. An additional sample was obtained without forced convective drying (ND) and employed to extract alginates from the UAE wet residue. ND sample was immediately subjected to alginate extraction without additional storage time. Commercial alginate (CA) was employed as reference.

2.3. Alginates extraction

Sodium alginates from UAE solid pellets were obtained following the methodology reported by Chee S et al. (2011). Briefly, the solid was soaked in $CaCl_2$ solution (1% *w*/w) with constant liquid/solid (L/S) ratio (15 kg of solvent/kg of dried pellet, kg_s/kg_{DR}). This blend was stirred at 150 rpm for 18 h at rt. The supernatant was discarded and the solid was washed 3-times with double-distilled water, maintaining the solvent-to-solid ratio constant and discarding all supernatants. Then, the solid particles were soaked in acid solution (HCl, 5% w/w), at the same

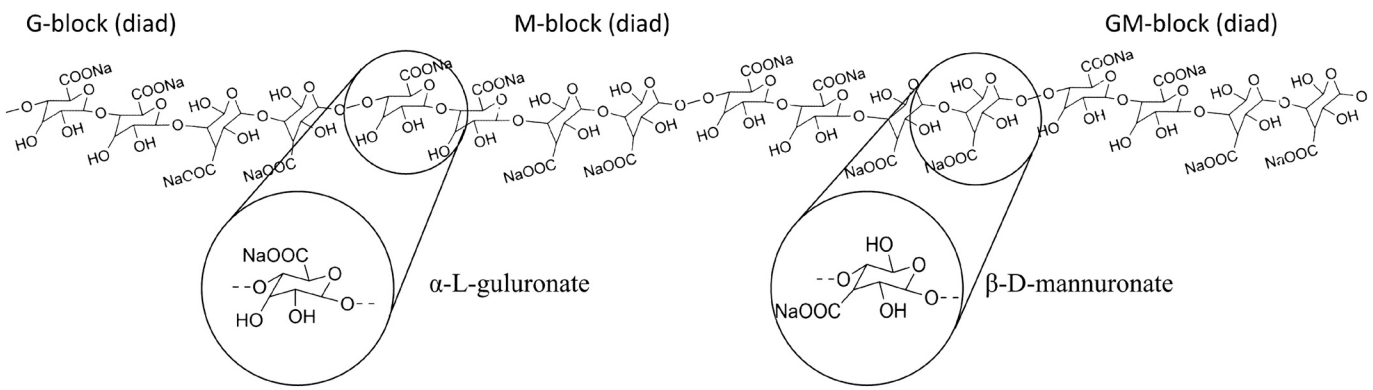

Fig. 1. Molecular structure of sodium alginate, their components: α-L-guluronate (G) and β-D-mannuronate (M) and diad structures GG, MM and GM-blocks.

above-mentioned L/S ratio and stirring, for 1 h at rt. After acidic treatment 3 washes with double distilled water were carried out. Solid residue was decanted and blended with alkaline solution (Na_2CO_3, 3% w/w) again at the same L/S and stirring for 1 h. After sodium carbonate treatment, distilled water was added to the solid (L/S of 12.5 kg_s/kg_{DR}) and rested for 8 h at rt. The viscous blend was separated from solid residue by centrifugation at 8500 ×*g* for 5 min. Sodium alginate was precipitated adding ethanol-water solution (50%, *v*/v) with 1:1 (*v*/v) liquid-liquid ratio. Sodium alginates fibres were filtered, washed carefully with ethanol (96%, v/v), aired for 24 h and finally dried at 50 °C during 2.5 h up to 9.1 ± 0.2% d.s. Dried alginate samples were milled and stored at rt. until use. The extraction yield was calculated and expressed as kg alginates per 100 kg of dried seaweed (Mohammed et al., 2020).

2.4. Structural characterization: FT-IR and NMR

Fourier transform infrared spectrophotometry (FT-IR) was applied to characterise the alginates molecular composition. FT-IR spectra were recorded with a Bruker FT-MIR model Vertex 70 V spectrometer. Wave number range was in the range 4000 to 50 cm^{-1}. All alginate powder samples were blended with KBr and compressed into disks. FT-IR spectra treatment was carried out with Omnic 7.1 software (Thermo Scientific, USA). FT-IR data were supplemented by elemental analysis (CHNS) carried out with a Thermo Finnigan (Flash 1112 model) elemental analyser.

Proton nuclear magnetic resonance spectroscopy (^{1}H NMR) spectra were collected with Bruker NEO 750 spectrophotometer operated with a 17.61 T (750 MHz resonance ^{1}H) magnetic field strength. Alginate samples were blended with D_2O. ^{1}H NMR spectroscopy was used to analyse composition and mannuronic block (M) and glucuronic block (G) distribution into monads (F_M and F_G), diads (F_{GG}, F_{MM}, F_{MG}, F_{GM}) and triads (F_{GGG}, F_{MGM}, F_{GGM}), M/G ratio and block average length ($N_{G>1}$) from sodium alginates samples, following ASTM standard F2259-10 (ASTM, 2012). ^{1}H-RMN spectra peaks integration was carried out with MestreNova software (Mestrelab Research, Spain).

2.5. Capillary viscometry: viscosity average molecular weight

Several solutions of extracted alginates, from 0.025 up to 3% *w/v*, were prepared. Neutral alginate solutions were obtained (pH from 6.8 to 7.0). The determination of the kinematic viscosity (ν) was performed using a Ubbelohde viscometer (AVS 350, Schott-Geräte, GmbH, Germany) using an aqueous NaCl 0.1 M solution as solvent. This salt content is above threshold concentration (0.025 mol/L) to assume alginate in a random coil conformation (Dodero, Vicini, Alloisio, & Castellano, 2020). For each sample, five measurements were taken at 25 °C (±0.1 °C). Density, ρ, was determined by pycnometry (at least four replicates) at 25 °C (±0.1 °C) to obtain the corresponding absolute viscosity ($\mu = \nu\ \rho$) values. A linear relationship ($r^2 > 0.99$) between density (g/cm^3) and alginate concentration (C, g/dL), was found to be $\rho = 1.0038 + 0.0061C$. With the absolute viscosity of the solvent (μ_0) and alginate (μ) solutions, the relative viscosity (μ_r) and the specific viscosity (μ_{sp}) were calculated by: $\mu_r = \mu/\mu_0$ and $\mu_{sp} = \mu_r - 1$. The viscosity average molecular weight ($\overline{M}_v$, g/mol) was determined by the Mark-Houwink equation (Eq. (1)):

$$[\mu] = K\,\overline{M}_v^{\alpha} \tag{1}$$

where $[\mu]$ (dL/g) is the intrinsic viscosity. K and α values depend on the solute-solvent system at constant temperature and only for a range of molecular weights. In this study, the intrinsic viscosity $[\mu]$ was evaluated by the Huggins and Kraemer and the Fedors methods (Dodero, Vicini, & Castellano, 2020).

To determine $[\mu]$ using the Huggins and Kraemer method, the values of reduced ($\mu_{red} = \mu_{sp}/C$) and inherent ($\mu_{inh} = \ln(\mu_r)/C$) viscosity were calculated and plotted against alginate concentration (g/dL). By linear regression of the experimental data and through the Huggins (Eq. (2)) and Kraemer (Eq. (3)) equations, the values of $[\mu]$ and of the Huggins (K_H) and Kraemer (K_K) constants were calculated.

$$\mu_{red} = [\mu] + K_H\,[\mu]^2\,C \tag{2}$$

$$\mu_{inh} = [\mu] + K_K\,[\mu]^2\,C \tag{3}$$

The Fedors equation (Eq. (4)) is valid for polymer solutions in the dilute and semi-dilute ranges and the application range is restricted by the μ_r values (between 1 and 100). The $[\mu]$ is calculated by:

$$\frac{1}{2\left(\mu_r^{0.5} - 1\right)} = \frac{1}{C\,[\mu]} - \frac{1}{C_{max}[\mu]} \tag{4}$$

where C_{max} (g/dL) is the theoretical concentration at which the interactions between polymer molecules are considered very significant.

2.6. Rheological characterization

All rheological measurements were performed using an Anton Paar-Physica MCR 301 Rheometer (Graz, Austria) equipped with a Peltier heating system (±0.01 °C) and a solvent trap kit to minimize water evaporation during tests. Couette geometry (CC24-SN40990) was used with a gap of 1 mm. Flow curves were carried out in a wide shear rates range of 0.1 to 1000 s^{-1} (upwards) and of 1000 to 0.1 s^{-1} (downwards) to determine the existence of thixotropic behaviour at 25 °C. Three concentration values were used for each tested alginate corresponding to 2C*, 4C* and 6C*, where C* is the overlap concentration from dilute to semi-dilute regime. On the other hand, only the concentration of 6C* was used to determine the viscoelastic characteristics of solutions by small amplitude oscillatory shear (SAOS) tests. Amplitude sweep tests were performed in the strain range from 0.1 to 10% and at constant frequency (1 Hz) and temperature (25 and 45 °C) to obtain the linear viscoelasticity range (LVR). Frequency sweep tests were performed in the range from 0.01 to 10 Hz at a constant strain (1%) and temperature (25 and 45 °C).

2.7. Statistical analysis

Statistical analysis was carried out by IBM SPSS statistics 24 (SPSS Inc., USA) software. A one-way analysis of variance (ANOVA) was assessed based on confidence interval of 95% ($p < 0.05$) using Duncan test. Data collected ^{1}H NMR, FT-IR, viscometry, and rheology tests were treated and plotted on MATLAB R2019b software (MathWorks Inc., USA) and Microsoft Excel (Microsoft Corporation, USA). All experimental results were expressed as mean ± standard deviation from at least from triplicate experiments.

3. Results and discussion

Extraction yield (%) of alginates from UAE undried (ND) and dried (50D and 90D) solids varied significantly ($p < 0.05$) with employed pellet drying conditions, 20.3 ± 0.9, 23.7 ± 0.5 and 18.3 ± 0.4, respectively. Maximum yield was achieved after drying of pellet at 50 °C and is comparable to that reported (24%) by Rioux et al. (2007)) working with *Ascophyllum nodosum* (AN) and is also in the range (from 20 to 41%) reported for other brown seaweeds (Chee S et al., 2011). The yield after drying at 90 °C dramatically decreased due to probably alginates losses from solid (by solubilization) during processing. The low yield at rt. may be justified by a dilution effect due to the presence of the water that initially accompanies the solid and that diminishes the effect of the treatments.

3.1. Structural characterization: FT-IR

FT-IR spectra corresponding to extracted alginates from UAE undried (ND) and dried (50D and 90D) solids and CA are shown in Fig. 2. Sodium alginates presented the characteristic bands up 4000 to 600 cm^{-1} range (Gómez-Ordóñez & Rupérez, 2011). The peak between 3600 and 3200 cm^{-1} corresponded to stretching vibrations of O—H bonds. The 2930 cm^{-1} peak were stretching vibrations of C—H bonds. These peaks at 4000–2000 region are common to polysaccharides (El Atouani et al., 2016).

The peak range 1680–1620 cm^{-1} was ascribed to asymmetric stretching vibrations of carboxylic groups. The 1415 cm^{-1} peak corresponded to deformation vibrations of C-OH bonds and asymmetric stretching vibrations of —C(=O)—O bonds (Mohammed et al., 2020). Around 1300 cm^{-1} peak appeared in the CA, but not in the AN extracted alginate. Literature refers this peak to S=O bond from sulphated polysaccharides such as fucoidans also extracted from marine brown seaweed (Gómez-Ordóñez & Rupérez, 2011). The lack of this peak seemed to indicate the absence or low concentration of sulphated carbohydrates in the extracted alginates (Blanco-Pascual et al., 2014). Elemental analysis results (CHNS) confirmed this result, where higher sulphur content (0.09%) in CA than in 50D, 90D and ND samples (0.05, 0.01 and 0.02%, respectively) was determined.

The observed peak in the range 1091–1031 cm^{-1} corresponded to deformation vibrations of C—C—H and O—C—H bonds, stretching vibrations of C—O bonds, and stretching vibrations of C—O and C—C bonds, present in alginate pyranose rings. The 1030 cm^{-1} was promoted by stretching vibrations of C—O bonds (Gómez-Ordóñez & Rupérez, 2011).

Three zones were observed in the range 950–750 cm^{-1}: firstly, 950 to 930 cm^{-1}, corresponding to C—O bonds stretching vibrations from uronic acid residues, secondly, 870 to 883 cm^{-1} corresponding to deformation vibrations of C—H bonds from mannuronic acids, and finally, 815–833 cm^{-1} region to stretching vibration also to C—H bonds (El Atouani et al., 2016).

No significant differences were observed between 50D, 90D and ND samples and minor differences with CA were observed, due to probably different seaweed species origin. Alginates extracted from solid subjected previously to UAE for polyphenols extraction of AN seaweeds showed structural features like commercial alginates. Further, the absence of additional peaks indicated a low level of impurities. This evidence was also supported by CHNS elemental analysis were pollutants as nitrogen or sulphur were under 1% and 0.1%, respectively.

3.2. Structural characterization: ^1H NMR

Structural features (monads, diads and triads) of commercial (CA) and extracted alginates from AN residue after polyphenols UAE that was undried (ND), dried at 50 °C (50D) and 90 °C (90D) evaluated from ^1H NMR spectra are summarised in.

Mannuronic content (F_M) of extracted alginates varied in a very narrow range (0.55 to 0.57) independently of drying conditions. Alginates from AN seaweed are characterized by their high mannuronic content in comparison to other seaweeds (Draget et al., 2006). Homopolymer diads blocks of samples presented higher F_{MM} values around 0.30–0.33, than F_{GG} values around 0.17–0.20. Heteropolymer blocks (F_{GM} or F_{MG}) content ranged from 0.23 to 0.26. F_{GGG} triads content ranged from 0.06 (ND) to 0.11 (90D), F_{MGM} and F_{GGM} did not show differences among extracted samples being around 0.15 for extracted alginates. Average block size ($N_{G>1}$) varied from 1.97 (90D) up to 2.15 (ND). Dried samples (50D and 90D) shower lower $N_{G>1}$ values than undried (ND) sample. M/G ratio varied from 1.21 (50D) to 1.33 (90D and ND). As expected, these results indicated that drying of UAE residue did not modify significantly to monads, diads and triads distribution of

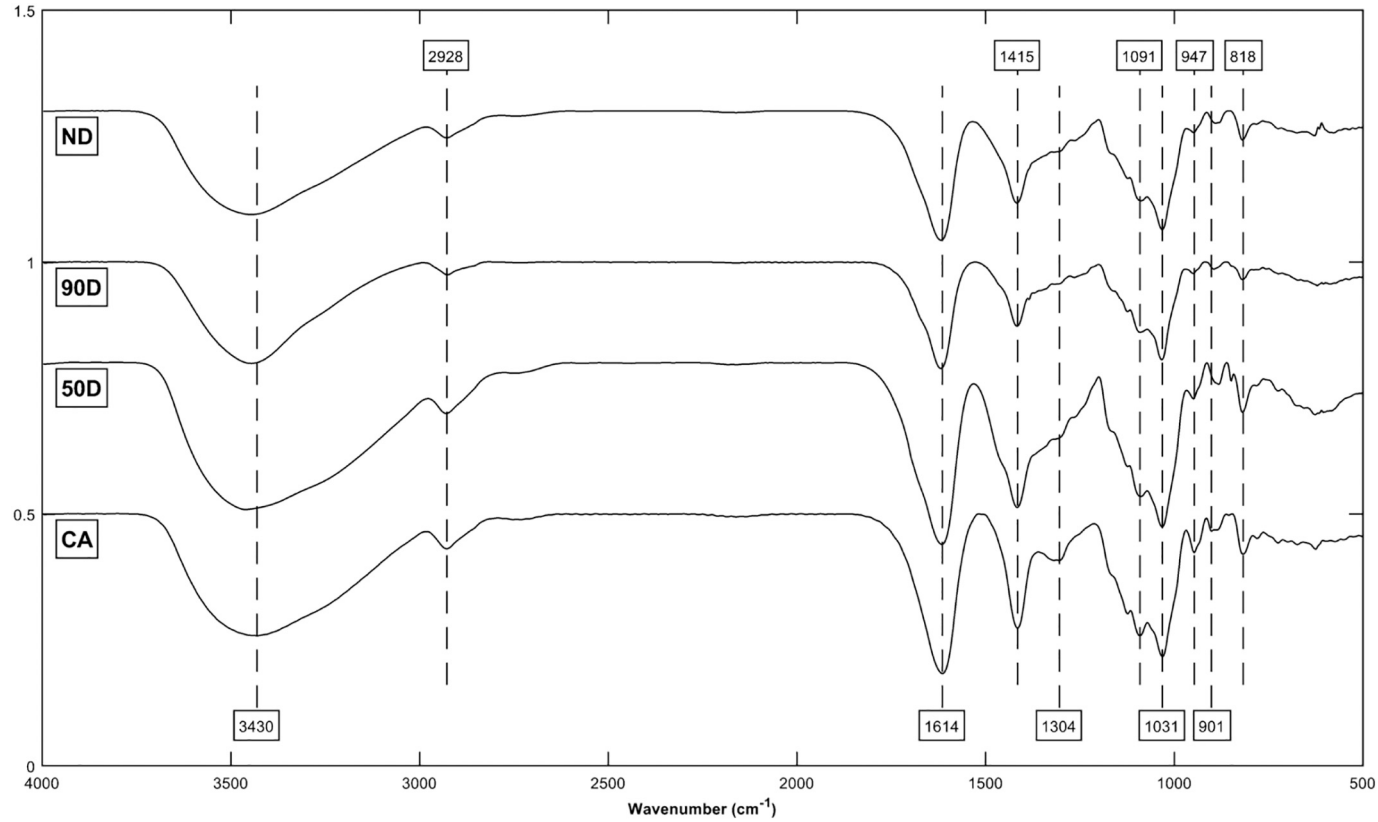

Fig. 2. FT-IR spectra of commercial alginate (CA) and extracted alginate from *Ascophyllum nodosum* sonication residue not dried (ND) and dried at 50 °C (50D) and 90 °C (90D), showing main characteristic absorption bands of sodium alginate (–).

the alginates, but $N_{G>1}$ values seemed to decrease by increasing drying temperature. So, drying conditions must be carefully controlled to modulate final polymer structural features. Alginates with M/G ratios higher than one are suitable to produce elastic gels for food, cosmetical or pharmaceutical applications (Murillo-Álvarez & Hernández-Carmona, 2007).

In comparison to commercial alginate (CA), extracted alginates showed higher mannuronic contents (around 0.56) than CA (0.48). F_{MM} homopolymer content was similar, F_{MM} content of CA (0.35) was notoriously higher, and F_{GM} or F_{MG} (0.18) lower. F_{GGG} content was clearly higher for CA (0.30) than those determined for extracted alginates (0.09) and F_{MGM} and F_{GGM} showed minor differences from 0.12 to 0.15. $N_{G>1}$ value (3.30) of CA was notoriously higher than those of extracted alginates (< 2.15). Finally, M/G ratio of CA was lower than one (0.91) due to glucuronic fraction was predominant above mannuronic molecules.

The characteristics of extracted alginates were compared with those previously reported by other authors for alginates from AN. Authors employed different methods and conditions that are necessary to specify to compare results appropriately. In fact, Yuan and Macquarrie (2015) isolated alginates involving several steps at temperatures above 70 °C during short periods, however, the final alginates showed similar features to extracted alginates in this work, Table 1. Rioux et al. (2007) characterized dialyzed alginates (>1000 Da) with high average molecular weight. This fact could explain some differences with alginates studied here.

Mannuronic content (F_M) showed similar values and F_{MM} values were slightly lower than those (from 0.38 to 0.39) reported by other researchers (Donati & Paoletti, 2009; Yuan & Macquarrie, 2015), Table 1. Nevertheless, F_{MM} values were slightly higher than value (0.28) given by Rioux et al. (2007). F_{GG} and F_{GM} values agreed to ranges reported by other authors, Table 1. Regarding triads, the values were generally in accordance with ranges previously reported: F_{GGG} and F_{MGM} values agreed and F_{GGM} value was slightly higher than that (0.07) reported by Donati and Paoletti (2009). $N_{G>1}$ values were lower than data (5.0) found by Donati and Paoletti (2009). Higher value of M/G ratio (1.44) was reported than the range (1.22–1.33) determined from extracted alginates in this study, Table 1. Average block size differences could be related to different extraction methods and conditions (temperature-time) employed (Yuan & Macquarrie, 2015). Also, they can be attributed to seasonal variations and geographical origin of the seaweeds (Tabassum et al., 2016).

3.3. Capillary viscosimetry: viscosity average molecular weight

Fig. 3 shows the specific viscosity trend with alginate concentration for 50D, 90D and ND alginates extracted in this work and CA. Extracted alginates from AN showed two regime zones in the range of concentrations studied, while three regime zones were observed in CA. The determination of these zones is critical because different concentration regimes can be found. Models based on the intrinsic viscosity are highly sensitive to changes in concentration regime.

Through the intersection of the straight lines, overlap concentration C* (transition from dilute to semi-dilute regime) values were obtained for the four alginates tested. The C* values were 0.25 ± 0.01, 0.46 ± 0.02, 0.52 ± 0.03 and 0.52 ± 0.03 g/dL for ND, 50D, 90D and CA, respectively. From C* values, only significant differences for ND (undried solid) were observed. Dodero, Vicini, Alloisio, and Castellano (2020) reported for low molecular weight alginates (~100 kg/mol) C* values of 0.60 ± 0.1 g/dL, in the same range of concentration showed by extracted alginates with drying step. Moreover, the concentration value of the transition from semi-dilute to concentrated regime, C** in CA was 1.08 ± 0.11 g/dL.

Once the regimes were determined, the Huggins, Eq. (2), Kraemer, Eq. (3), and Fedors, Eq. (4), equations were applied to determine [μ] of each alginate. The Huggins and Kraemer equations were applied to correlate the data obtained in the diluted regime (C < C*). The values of k_H and k_K were determined from the slopes of both equations and [μ] was obtained from the intercept. The Fedors equation is applicable in both dilute and semi-dilute regimes and [μ] and C_{max} could be obtained. Mark-Houwink equation, Eq. (1), relates [μ] with the viscosity average molecular weight. The K and α values used for extracted alginates were $4.84{\cdot}10^{-5}$ dL/g and 0.97 previously evaluated for AN alginates (Stokke et al., 2000), and the K and α values used for CA were $7.30{\cdot}10^{-5}$ dL/g and 0.92 (Martinsen et al., 1991). The results obtained are collected in Table 2.

The parameters of the Huggins and Kraemer equations, k_H and k_K, varied in a narrow range (from 0.30 to 0.42 and from −0.15 to −0.12, respectively), Table 2. In fact, no significant differences in the k_H values were observed and only statistical differences were found in k_K between ND, CA and 50D, 90D alginates. From statistical analysis, regarding C_{max} of the Fedors equation, no significant differences between 50D, 90D and CA alginates were found and lower values for ND alginates were found. On the other hand, both methods reported similar [μ] values (also for M_v) decreasing significantly with the existence of a drying step and with increasing drying temperature. No significant differences between 90D and CA were found. M_v (kg/mol) values obtained for extracted alginates from AN, varied in a wide range from 133.3 (90D) and 427.8 (ND). These results indicate clearly that molecular size of extracted alginates can be modulated by the use and conditions employed during drying conditions. M_v determined for CA (156.1 kg/mol) is close to that determined for 90D. Despite different seaweed origin and other aspects, it could be probably related to the severe industrial conditions employed during extraction process. The molecular weights obtained are within

Table 1
Structural features of commercial alginate (CA) and extracted alginates undried (ND) and dried at 50 °C (50D) and 90 °C and (90D) and comparison with alginates extracted from *Ascophyllum nodosum* (AN) seaweeds by other authors.

	This study				Yuan and Macquarrie (2015)	Donati and Paoletti (2009)	Rioux et al. (2007)
Seaweed	Unknown	AN	AN	AN	AN	AN	AN
Alginate	CA	50D	90D	ND			
F_M	0.48	0.55	0.57	0.57	0.59	0.59	0.46
F_G	0.52	0.45	0.43	0.43	0.41	0.41	0.54
F_{MM}	0.30	0.30	0.33	0.31	0.39	0.38	0.28
F_{GG}	0.35	0.20	0.20	0.17	0.21	0.22	0.36
$F_{GM} = F_{MG}$	0.18	0.25	0.23	0.26	0.21	0.21	0.18
F_{GGG}	0.30	0.10	0.11	0.06		0.13	
F_{MGM}	0.12	0.15	0.15	0.14		0.14	
F_{GGM}	0.12	0.15	0.15	0.14		0.07	
$N_{G>1}$	3.30	2.07	1.97	2.15		5.00	
M/G	0.91	1.21	1.31	1.33	1.44	1.44	1.44

Mannuronate (M) and guluronate (G); $N_{G>1}$: average block length; F_M: M fraction; F_G: G fraction; F_{MM}, and F_{GG}: homopolymer fraction diads; F_{GM}: heteropolymer fraction diads; F_{GGG} and F_{MMM} homopolymer fraction triads; F_{MGM} and F_{GGM}: heteropolymer fraction triads.

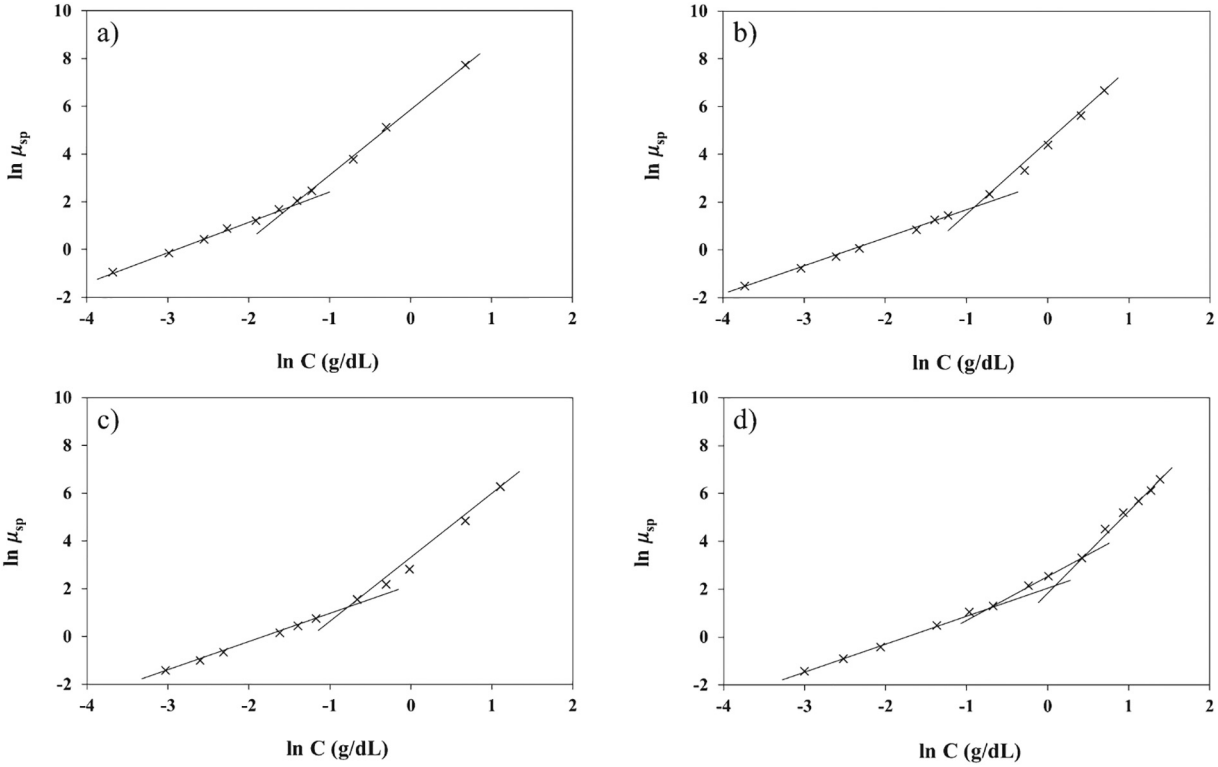

Fig. 3. Specific viscosity (μ_{sp}) vs concentration (C, g/dL), both in logarithmic scale, for different alginates: a) ND, b) 50D, c) 90D and d) CA.

Table 2
Parameters obtained from the Huggins and Kraemer and Fedors (Eqs. (2 to 4)) equations of commercial alginate (CA) and extracted alginate undried (ND), dried at 50 (50D) and 90 °C (90D).

Sample	Huggins and Kraemer				Fedors		
	k_H	k_K	[η] (dL/g)	M_v (kg/mol)	C_{max} (g/dL)	[η] (dL/g)	M_v (kg/mol)
ND	0.30 ± 0.02^{b}	−0.12 ± 0.01^{b}	14.06 ± 0.16^{c}	427.8 ± 7.2^{d}	1.46 ± 0.17^{a}	14.05 ± 0.18^{c}	427.7 ± 8.3^{d}
50D	0.25 ± 0.12^{a}	−0.14 ± 0.01^{a}	8.58 ± 0.03^{b}	257.3 ± 1.2^{c}	6.21 ± 0.58^{b}	8.73 ± 0.02^{b}	262.0 ± 1.1^{c}
90D	0.36 ± 0.16^{a}	−0.15 ± 0.01^{a}	5.03 ± 0.52^{a}	133.3 ± 1.2^{b}	5.44 ± 0.81^{b}	4.65 ± 0.02^{a}	136.8 ± 1.0^{b}
CA	0.42 ± 0.12^{a}	−0.12 ± 0.01^{b}	4.38 ± 0.02^{a}	156.1 ± 1.5^{a}	5.77 ± 0.05^{b}	4.54 ± 0.36^{a}	162.9 ± 0.2^{a}

Data are presented as mean ± standard deviation. Data value of each parameter with different superscript letters are significantly different ($p \leq 0.05$).

the usual ranges reported for commercial alginates (Dodero, Vicini, & Castellano, 2020). Similarly, Chen et al. (2021) determined molecular weights of several brown seaweeds (*Sacharina japonica*, *Undaria pinnatiufida*, *Sargassum fusiforme* and *Sargassum hemiphyllum*) ranging from 171.8 to 663.0 kg/mol.

The Huggins and Kraemer constants provided information about the interactions between polymer-polymer and polymer-solvent molecules. Thus, k_H values lower than 0.5 (range 0.25–0.42) were characteristic of flexible macromolecules and together with negative k_K values (range −0.15 and −0.12) indicated strong polymer-solvent and polymer-polymer weak interactions with a random coil conformation (Da Costa et al., 2017). The obtained values agreed with those reported by other authors for other carbohydrate polymers (Chenlo, Moreira, & Silva, 2009).

The normalized master curve was obtained by plotting (log-log) the μ_{sp} data of each alginate versus dimensionless concentration or Berry number (C [η]). This normalized concentration measures the degree of occupation of the polymer in the solution (Castelain et al., 1987). At low dimensionless concentrations, μ_{sp} increased linearly with [η] up to achieve a critical concentration (C_{cr}) where the slope increased sharply. C_{cr} defines the change from dilute to semi-dilute regime, where the interactions between polymer molecules begin to be significant. Fig. 4 shows the acceptable normalized master curve of the tested alginates where C_{cr} was 4.05 which was consistent with the values found in literature (Benaoun et al., 2017; Lopez et al., 2020). The slopes obtained were 1.4 and 2.9 in the diluted and semi-diluted concentration range, respectively. These values agreed with those reported by other authors for other polysaccharide solutions (Hellebois et al., 2021).

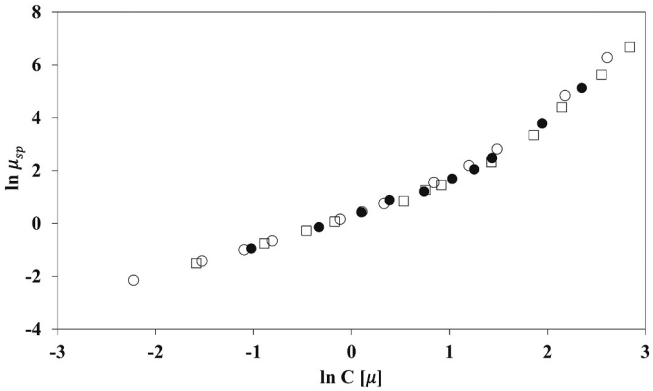

Fig. 4. Master curve, μ_{sp} vs C [μ], for NS (●), 50D (□) 90D (○).

3.4. Rheological characterization

3.4.1. Steady-shear flow properties

The viscous properties for aqueous alginate solutions at different concentrations (2C*, 4C* and 6C*) at 25 °C were determined using steady-shear flow test over the range of shear rate from 0.1 to 1000 s^{-1}. Upwards and downwards steady-shear flow curves were coincident in all cases indicating that alginate solutions, in the range of tested polymer concentration, were not dependent on time (no thixotropic nor rheopectic behaviour). Flow curves showed two trends as function of shear rate, Fig. 5. At low shear rates, apparent viscosity value remained constant regardless of the shear rate value (Newtonian plateau). Above a determined shear rate, critical shear rate ($\dot{\gamma}_c$), apparent viscosity decreased (shear-thinning behaviour). This behaviour has been already described for alginate solutions (Ma et al., 2014; Rezende et al., 2009). The plateau tended to increase with decreasing M_v or C affecting the determination of $\dot{\gamma}_c$. In fact, studied alginate of lower M_v (90D) at the lowest tested concentration 2C* can be considered Newtonian. The existence of different range of the Newtonian plateau is attributed to the variation in the formation-breakage equilibrium of entanglements between alginate molecules (Doyle et al., 2009). The apparent viscosity of solutions increased noticeably with increasing alginate concentration forming viscous solutions, being this effect one of the most important properties of alginates for many industrial applications (Draget et al., 2006).

The Cross-Williamson model (Morrison, 2001) was employed to model the flow curves, Eq. (5):

$$\mu = \frac{\mu_0}{1 + K\,\dot{\gamma}^{(1-n)}} \tag{5}$$

where μ (Pa s) is the apparent viscosity, μ_0 (Pa s) is the viscosity in the Newtonian regime, K is the consistency index, $\dot{\gamma}$ (s^{-1}) is the shear rate and n is the flow index. The μ_0 decreased linearly with increasing absolute temperature, T_D (K), of drying stage (ND temperature was assumed 293.1 K), $\mu_0 = A + B\,T_D$. A and B parameters showed an exponential trend with C/C* ratio. Moreover, K was related to drying temperature by means of an exponential relationship, $K = D\,e^{-E\,T_D}$, and parameter D was linearly correlated with C/C* ratio. Finally, flow index varied in a narrow range (from 0.28 to 0.30) and was considered constant (0.29). Eq. (6) was able to reproduce the apparent viscosity in the range of tested alginate concentration and temperature of drying stage (mean relative error of 16% and $r^2 > 0.95$). Fig. 5 shows the quality of fitting for 50D and 90D samples at different alginate concentrations, as example.

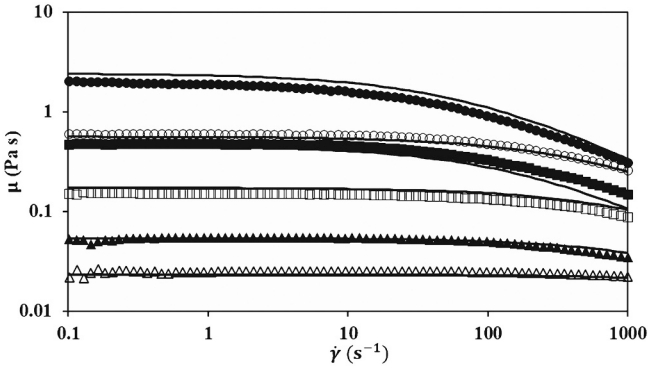

Fig. 5. Steady-shear flow curves for 50D (filled markers) and 90D (hollow markers) alginate solutions, experimental data for 2C* (●, ○), 4C* (■, □) and 6C* (▲, △) and model data. Eq. (6) (-).

$$\mu = \frac{\left(0.05 - 1.29\ 10^{-4}\ T_D\right)\ e^{\left(\frac{C}{C^*}\right)}}{1 + \left(4365\left(\frac{C}{C^*}\right) - 7494\right)\ e^{-0.04\ T_D}\dot{\gamma}^{0.71}} \tag{6}$$

3.4.2. Viscoelastic properties

Frequency sweep was carried out at constant strain (1%), inside LVR previously determined with corresponding strain sweeps at high frequency, varying frequency from 0.1 to 10 Hz at 25 and 45 °C with alginate solutions at 6C* concentration. In all cases, elastic (G′) and viscous (G″) modules increased with increasing frequency and, in all cases, G″ > G′ (liquid-like behaviour) (Fig. 6). Different trends of G″ and G′ slopes with frequency were observed between samples at 25 °C. ND alginate solution showed G″ slope higher than G′ slope achieving at 10 Hz a tan δ of 1.72 near to gel point (G′ = G″), G″ and G′ slopes were similar in 50D sample and, finally, G′ slope was higher than G″ slope for 90D sample. Ma et al. (2014) reported the same behaviour for commercial sodium alginate solutions in a similar range of concentrations and M_v.

As expected, both viscoelastic modules decreased with temperature (from 25 to 45 °C) in the cases of 50D and 90D alginate solutions. Nevertheless, ND alginate showed a different behaviour at 45 °C where G′ was invariant with the increase of temperature and G″ notably increased at low shear rates (below 1 Hz). In fact, at 0.03 Hz G′ (0.48 Pa) was close to G″ (0.67 Pa), tan δ = 1.39, indicating that higher temperatures could allow the gel point achievement of this alginate solution (Steffe, 1996). This behaviour is typical of semi-dilute polymer solutions that show a high degree of entanglement (Mohammadifar et al., 2006). This result seemed to indicate that solutions with high M_v alginates have low gelation temperatures.

The relationship between steady-shear flow and dynamic-shear rheology can be established by means of Cox-Merz rule, where apparent viscosity obtained with rotational tests and complex viscosity (μ^*) obtained with oscillatory tests are coincident. Fig. 7 shows the application of this rule to tested alginate solutions. In general, the Cox-Merz rule was satisfactorily accomplished for 50D and 90D solutions where the superposition of both viscosity curves was obtained independently of shear rate range. In the case of ND solution, only at high shear rates (>10 s^{-1}) the superposition was observed, and at low shear rates (<10 s^{-1}) dynamic viscosity was clearly higher than complex viscosity. Despite all these tests are performed at high polymer concentration (6C*), the concentration of ND samples is around 1.5 g/dL that is near C_{max} evaluated by Fedors equation where interactions between polymers are already important (concentrated regime). In the rest of the cases, the concentration employed (3 g/dL) is clearly lower than C_{max} and solutions can be considered inside the semi-dilute range. The existence of strong polymer interactions and entanglements in ND solutions promoted by its high viscosity average molecular weights could explain the observed divergence. Ahmad et al. (2014)) also observed a similar behaviour for guar galactomannan solutions and gellan/dextran blends with weak-gels characteristics.

4. Conclusions

Structural analyses showed that the extracted sodium alginates from *Ascophyllum nodosum* seaweeds after UAE of polyphenols presented low level of impurities. Intermediate drying of solid pellet between polyphenols and alginates extraction operations affected mainly to average block length and the viscosity average molecular weight evaluated by means of both Huggins-Kraemer and Fedors models with very good fitting. In fact, both properties decreased with drying temperature. Rheological properties of sodium alginate solutions depended on the drying stage and its thermal conditions. Solutions in the semi-dilute regime showed a shear-thinning behaviour and Cross-Williamson

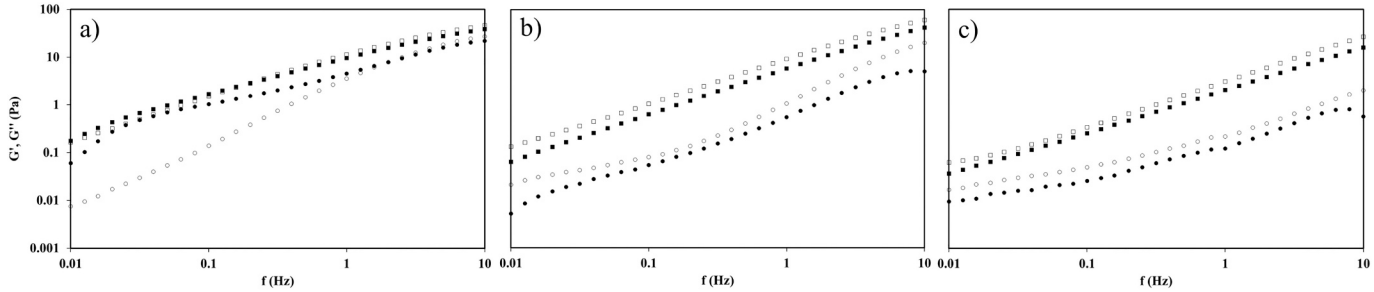

Fig. 6. Frequency sweeps of alginate solutions at 6C* concentration: experimental data of G″ (□, ■) and G′ (○, ●) at 25 °C (hollow markers) and 45 °C (filled markers) for different alginates: a) ND, b) 50D and c) 90D.

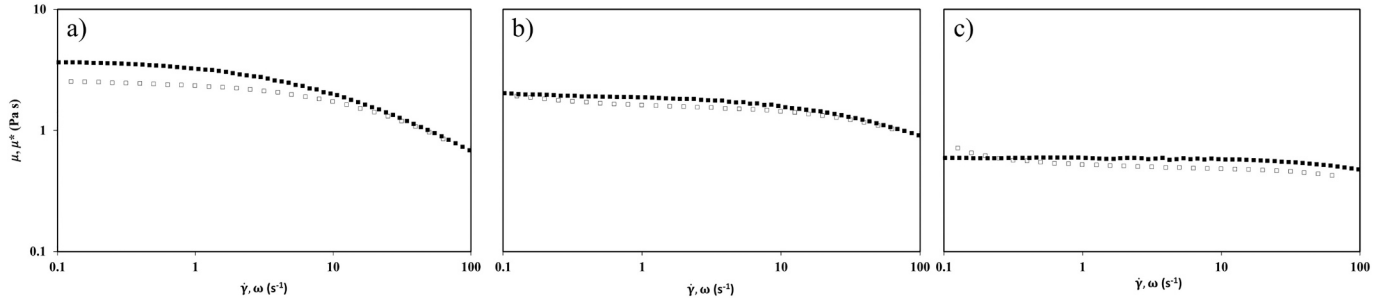

Fig. 7. Cox-Merz plot: Dynamic viscosity, μ, (■) and complex viscosity, μ*, (□) at 25 °C of alginate solutions at 6C* concentration for different alginates: a) ND, b) 50D and c) 90D.

model was adequate to estimate the apparent viscosity as function of polymer concentration and temperature employed for pellet drying. Liquid-like behaviour was determined by viscoelasticity tests, but alginate solutions with higher viscosity average molecular weight showed a trend to achieve a gel point with temperature. Cox-Merz rule was satisfied for alginate solutions at semi-dilute regime, but samples evaluated at concentrated regime showed significant differences with steady shear viscosities higher than complex viscosities by its enhanced elastic trend.

A sequential extraction that comprises the extraction of polyphenols with ultrasound technology (to decrease the time of operation and avoiding the use of organic solvents) followed with controlled drying conditions previously to the extraction of alginates allows to obtain them with different properties that can be modulated according to demand. The integral use of a raw material, like seaweeds, implies clear economic and environmental advantages obtaining multiple products of industrial interest.

Funding statement

This work was supported by the Ministry of Science and Innovation of Spain and European Regional Development Fund (ERDF) of European Union by the research project (RTI2018-095919-B-C2) and Xunta de Galicia, Spain (Consolidation Project ED431B 2019/01).

CRediT authorship contribution statement

Leticia Montes: Methodology, Validation, Formal analysis, Investigation, Writing – original draft. **Mauro Gisbert:** Methodology, Validation, Formal analysis, Investigation, Writing – original draft. **Ignacio Hinojosa:** Formal analysis, Investigation. **Jorge Sineiro:** Methodology, Writing – review & editing, Supervision. **Ramón Moreira:** Conceptualization, Methodology, Writing – review & editing, Supervision, Funding acquisition.

Declaration of competing interest

The authors declare no conflict of interest.

References

Ahmad, N. H., Ahmed, J., Hashim, D. M., Manap, Y. A., & Mustafa, S. (2014). Oscillatory and steady shear rheology of gellan/dextran blends. *Journal of Food Science and Technology, 52*, 2902–2909.

ASTM. (2012). ASTM F2259-10. In *Standard test method for determining the chemical composition and sequence in alginate by proton nuclear magnetic resonance (^{1}H NMR) spectroscopy*. West Conshohocken, PA: American Society for Testing and Materials.

Benaoun, F., Delattre, C., Boual, Z., Ursu, A. V., Vial, C., Gardarin, C., … Pierre, G. (2017). Structural characterization and rheological behavior of a heteroxylan extracted from *Plantago notata Lagasca* (Plantaginaceae) seeds. *Carbohydrate Polymers, 175*, 96–104.

Blanco-Pascual, N., Montero, M. P., & Gómez-Guillén, M. C. (2014). Antioxidant film development from unrefined extracts of brown seaweeds *Laminaria digitata* and *Ascophyllum nodosum*. *Food Hydrocolloids, 37*, 100–110.

Castelain, C., Doublier, J., & Lefebvre, J. (1987). A study of the viscosity of cellulose derivatives in aqueous solutions. *Carbohydrate Polymers, 7*, 1–16.

Chee, S. Y., Wong, P. K., & Wong, C. L. (2011). Extraction and characterisation of alginate from brown seaweeds (Fucales, *Phaeophyceae*) collected from Port Dickson, Peninsular Malaysia. *Journal of Applied Phycology, 23*, 191–196.

Chen, S., Sathuvan, M., Zhang, X., Zhang, W., Tang, S., Liu, Y., & Cheong, K. L. (2021). Characterization of polysaccharides from different species of brown seaweed using saccharide mapping and chromatographic analysis. *BMC Chemistry, 15*, 1.

Chenlo, F., Moreira, R., & Silva, C. (2009). Rheological modelling of binary and ternary systems of tragacanth, guar gum and methylcellulose in dilute range of concentration at different temperatures . *LWT - Food Science and Technology, 42*, 519–524.

Cotas, J., Leandro, A., Monteiro, P., Pacheco, D., Figueirinha, A., Gonçalves, A. M. M., … Pereira, L. (2020). Seaweed phenolics: From extraction to applications. *Marine Drugs, 18*, 384.

Da Costa, M., Delpech, M., Ferreira, I., Cruz, I., Castanharo, J., & Cruz, J. (2017). Evaluation of single-point equations to determine intrinsic viscosity of sodium alginate and chitosan with high deacetylation degree. *Polymer Testing, 63*, 427–433.

Dodero, A., Vicini, S., & Castellano, M. (2020). Depolymerization of sodium alginate in saline solutions via ultrasonic treatments: A rheological characterization. *Food Hydrocolloids, 109*, 106–120.

Dodero, A., Vicini, S., Alloisio, M., & Castellano, M. (2020). Rheological properties of sodium alginate solutions in the presence of added salt: An application of Kulicke equation. *Rheologica Acta, 59*, 365–374.

Donati, I., & Paoletti, S. (2009). Material properties of alginates. In B. Rehm (Ed.), *Alginates: Biology and applications*. Berlin: Springer.

Doyle, J., Lyons, G., & Morris, E. (2009). New proposals on "hyperentanglement" of galactomannans: Solution viscosity of fenugreek gum under neutral and alkaline conditions. *Food Hydrocolloids, 23*, 1501–1510.

Draget, K., Moe, S., Gudmund, S., & Olav, S. (2006). Alginates. In A. Stephen, G. Phillips, & P. Williams (Eds.), *Food polysaccharides and their applications* (pp. 289–334). London: Taylor & Francis.

El Atouani, S., Bentiss, F., Reani, A., Zrid, R., Belattmania, Z., Pereira, L., Mortadi, A., Cherkaoui, O., & Sabour, B. (2016). The invasive brown seaweed *Sargassum muticum* as new resource for alginate in Morocco: Spectroscopic and rheological characterization. *Phycological Research, 64*, 185–193.

Gómez-Ordóñez, E., & Rupérez, P. (2011). FTIR-ATR spectroscopy as a tool for polysaccharide identification in edible brown and red seaweeds. *Food Hydrocolloids, 25*, 1514–1520.

Hellebois, T., Soukoulis, C., Xu, X., Hausman, J.-F., Shaplov, A., Taoukis, P. S., & Gaiani, C. (2021). Structure conformational and rheological characterisation of alfalfa seed (*Medicago sativa* L.) galactomannan. *Carbohydrate Polymers, 256*, Article 117394.

Kadam, S. U., O'Donnell, C. P., Rai, D. K., Hossain, M. B., Burgess, C. M., Walsh, D., & Tiwari, B. K. (2015). Laminarin from Irish brown seaweeds *Ascophyllum nodosum* and *Laminaria hyperborea*: Ultrasound-assisted extraction, characterisation, and bioactivity. *Marine Drugs, 13*, 4270–4280.

Koivikko, R., Loponen, J., Honkanen, T., & Jormalainen, V. (2005). Contents of soluble, cell-wall-bound, and exuded phlorotannins in the brown alga *Fucus vesiculosus*, with implications on their ecological functions. *Journal of Chemical Ecology, 31*, 195–212.

Lopez, C. G., Voleske, L., & Richtering, W. (2020). Scaling laws of entangled polysaccharides. *Carbohydrate Polymers, 234*, Article 115886.

Ma, J., Lin, Y., Chen, X., Zhao, B., & Zhang, J. (2014). Flow behavior, thixotropy and dynamical viscoelasticity of sodium alginate aqueous solutions. *Food Hydrocolloids, 38*, 119–128.

Martinsen, A., Skjak-Braek, G., Smidsrod, O., & Paoletti, S. (1991). Comparison of different methods for determination of molecular weight and molecular weight distribution of alginates. *Carbohydrate Polymers, 15*, 171–193.

Mohammadifar, M., Musavi, S., Kiumarsi, A., & Williams, P. (2006). Solutions properties of targacanthin (water soluble part of gum tragacanth exudate from *Astragalus gossypinus*). *International Journal of Biological Macromolecules, 38*, 31–39.

Mohammed, A., Rivers, A., Stuckey, D. C., & Ward, K. (2020). Alginate extraction from Sargassum seaweed in the Caribbean region: Optimization using response surface methodology. *Carbohydrate Polymers, 245*, Article 116419.

Moreira, R., Chenlo, F., Sineiro, J., Arufe, S., & Sexto, S. (2016). Drying temperature effect on powder physical properties and aqueous extract characteristics of *Fucus vesiculosus*. *Journal of Applied Phycology, 28*, 2485–2494.

Morrison, F. (2001). *Understanding rheology*. New York: Oxford University Press.

Murillo-Álvarez, J. I., & Hernández-Carmona, G. (2007). Monomer composition and sequence of sodium alginate extracted at pilot plant scale from three commercially important seaweeds from Mexico. *Journal of Applied Phycology, 19*, 545–548.

Peteiro, C. (2018). Alginate production from marine macroalgae, with emphasis on kelp farming. In B. Rehm, & M. Moradali (Eds.), *Alginates and their biomedical applications* (pp. 27–66). Singapore: Springer.

Rezende, R., Bártolo, P., Mendes, A., & Filho, R. (2009). Rheological behavior of alginate solutions for biomanufacturing. *Journal of Applied Polymer Science, 113*, 3866–3871.

Rioux, L. E., Turgeon, S. L., & Beaulieu, M. (2007). Characterization of polysaccharides extracted from brown seaweeds. *Carbohydrate Polymers, 69*, 530–537.

Steffe, J. (1996). *Rheological methods in food process engineering* (2nd ed.). Michigan: Freeman Press.

Stokke, B. T., Draget, K. I., Smidsrød, O., Yuguchi, Y., Urakawa, H., & Kajiwara, K. (2000). Small-angle X-ray scattering and rheological characterization of alginate gels. 1. Ca-alginate gels. *Macromolecules, 33*, 1853–1863.

Tabassum, M. R., Xia, A., & Murphy, J. D. (2016). Seasonal variation of chemical composition and biomethane production from the brown seaweed *Ascophyllum nodosum*. *Bioresource Technology, 216*, 219–226.

Yuan, Y., & Macquarrie, D. J. (2015). Microwave assisted step-by-step process for the production of fucoidan, alginate sodium, sugars and biochar from *Ascophyllum nodosum* through a biorefinery concept. *Bioresource Technology, 198*, 819–827.